)

SPECTRAL VARIABILITY OF THE UNUSUAL AE HERBIG STAR V1295 AQL. I.

H. N. Adigozalzade [a*], ***U. Z. Bashirova*** [a], ***N. Z. Ismailov*** [a]

[a] *N.Tusi Shamakhy Astrophysical Observatory of Azerbaijan National Academy of Sciences, Shamakhy, Azerbaijan*

On the homogenous spectral observations obtained for May-September 2015 season we have obtained some new characteristics of spectral variability of the unusual Herbiq Ae star HD190073. It is shown that with an increasing of intensity in the blue absorption component in the profiles of hydrogen lines, the variability of the star's spectrum activated, which indicates the existence at this moment of an increasing in mass ejection from the disk. In a time interval of 98 days of observations, synchronous variability was discovered in these lines with a characteristic time of about 40 days. Monitoring of variations over time in the profiles of the emission components of the Hα and Hβ lines showed that the main variability in the lines occurs on the wings of individual components. The half-width (250 km/s) and full width (350 km/s) at the continuum level of the hydrogen emission lines probably indicate the existence of outflow and accretion of matter from the circumstellar disk.

Keywords: Pre-Main Sequence stars – circumstellar disks –variability – individual HD190073

1. INTRODUCTION

HD190073 (V1295 Aql, MWC325, A2IIIe - B9IIep+sh) is a very remarkable early-type object with emission lines in the visible spectrum. HD 190073 was variously classified as a peculiar Bep star [5] or as an evolved post main sequence A giant [12]. Recently HD190073 has gained recognition as a young Herbig Ae/Be star [10, 26]. In spite of being situated in the constellation of Aquila rather far from well-known regions of star formation, it displays a large far-IR excess due to thermal radiation of cool circumstellar (CS) dust [24]. The energy distribution of

)https://doi.org/10.59849/2078-4163.2024.1.6

* E-mail: hadigozalzade@gmail.com

HD190073 in this spectral region is similar to that of well known Herbig Ae stars, like AB Aur, HD 163296 and HD 31648 [19].

Alicia et al. [4] identified stellar parameters for V1295 Aql. Its magnetic field, ~ 100G, has been detected and confirmed by multiple authors over several years [1, 8, 14, 15]. As described in [4] from MIKE spectra RV $= -1.2 \pm 1.3$ km s^{-1} and v sin i $= 3.19 \pm 2.45$ km s^{-1}, consistent with [3]. Effective temperature is Teff $= 9250 \pm 250$ K, mass is M $= 2.9 \pm 0.5$M$_\odot$, radius is R $= 3.6 \pm 0.5$M$_\odot$. With these parameters and assuming star and disk share an inclination of $34^\circ \pm 2^\circ$ [18], they derive a rotation period of ~ 32 days. As noted in [2], the handful of observed magnetic HAeBe stars are also slow rotators, consistent with V1295 Aql's apparently very slow rotation rate. For the observations spanning multiple years [4], the P Cygni absorption is consistently growing weaker. In 2005 and 2006 dates blue shifted absorption is detectable in Hα, Hβ, Hγ, and Hδ, but can only be seen in Hα and Hβ thereafter; simultaneously, the emission component's EW is also growing weaker [4]. The Ca II infrared triplet is also dramatically weakening, as are the Na I D lines. The Ca II H and K lines, notable for their complex structure ([22], and references therein), are not seen to vary much on night to-night timescales, or within any given night. In the works [2, 3] were noted spectropolarimetric changes indicating V1295 Agl had a stable, aligned dipole over observations from 2004-2009, but in 2011-2012, variability was observed, indicating a change in the star's magnetic field structure [OI] 6300 Å in particular is of interest, as its driving mechanism remains unclear. Using multi-epoch data in the work [11] noted a relationship between the [OI] emission and the presence of near-IR excess; they suggested the IR excess was indicative of accretion. Line component analysis of [4] time-series data finds that the Hα wind absorption component is weakly anticorrelated with the [OI] emission: over the period of observation, the [OI] 6300 Å emission line grew stronger as the wind absorption in Hα grew weaker. The [OI] and [Ca II] lines show sharp, violet-shifted features [9, 13].Additionally, [Fe II] lines appear to be weakly present in emission.

Since in 2015 summary 22 nights of observations carried out during the period June-September, and this is the longest observation season, in first part of the work (article I) we will consider the variability of the star's spectrum for this year separately. In the second part (article II) we will present results of observations for 2016-2023 years and full analysis of the results of investigations.

2. OBSERVATIONS

Observations in 2015 were obtained with the Cassegrain Echelle Spectrograph (CES), which was created on the basis of the UAGS spectrograph [16, 17, 20]. As a detector was used a CCD matrix 530×580px, with size of pixels 24 mm devel-

oped at the Special Astrophysical Observatory (SAO) of the Russian Academy of Sciences. Observations were made in the λ range 4700-6700 Å. The CES spectrograph obtained a total of 22 pairs of spectrograms suitable for processing with a spectral resolution of 14000 . Observations in 2016-2023 carried out using the ShAO Fiber-Echelle Spectrograph (ShAFES), developed jointly by specialists from ShAO and SAO. A detailed description of the technical characteristics of this spectrograph is given in [21]. A CCD STA4150A (USA) with a size of 4096x4096px, with the size of pixel is 15 m, was used. The CCD cooled to a temperature of $-120°$C using liquid nitrogen. Spectral range $\lambda 3700 - 8000$ Å. Observations were performed with a combination of 2x2 pixels (binning), which allows to obtain a spectral resolution of $R = 28000$.

In just 8 years from 2015 to 2023, for 54 nights high-resolution echelle spectra have been obtained (Table 1). At each observation, spectra of the standard stars HR 7300 (Sp G8II-III) and HR 7734 (Sp F0V) were obtained. In all spectra, the signal to noise level on average reached $S/N = 80 - 100$ in the region of the Hα line. The errors in measuring radial velocities for standard stars were 1-1.5 km/s. Positional errors for spectrums with resolution 14000 nearly twice as large. The equivalent widths of the Balmer lines of hydrogen are determined with an precision less than $4 - 5\%$ and in intensities at 0.5%. The equivalent widths of absorption lines less than 0.4 Å was determined with errors at 10%.

Table 1. Obtained spectral material

Period	MJD Range	N	Range (Å)	Spectrograph	R	Mean Exposure (sec)
June 2015 - September 2015	57177.871 - 57275.813	22	4400-6700	CES	14000	900
June 2016 - September 2016	57581.938 - 57640.822	6	3700-8000	ShAFES	28000	1500
June 2017 - August 2017	57951.866 - 57978.781	7	3700-8000	ShAFES	28000	1500
June 2018 - August 2018	58300.871 - 58337.969	5	3700-8000	ShAFES	28000	2500
August 2019	58699.727 - 58719.802	5	3700-8000	ShAFES	28000	2500
June 2020 - August 2020	59034.942 - 59070.8	3	3700-8000	ShAFES	28000	2500
August 2021	59448.809	1	3700-8000	ShAFES	28000	2500
July 2022	59780.881	1	3700-8000	ShAFES	28000	3000
June 2023 - August 2023	60145.789 - 60178.8555	4	3700-8000	ShAFES	28000	3600

3. Hα AND Hβ LINES VARIABILITY IN 2015

As can be seen from Table 1, in 2015,22 nights of observations of the star carried out for June September (MJD 57177.871 - 57275.813). Some of preliminary results of this material published in our works [6, 7].

In the Fig.1, we have presented all profiles of the lines Hα and Hβ, obtained in 2015. The line Hα has one peak emission structure that superimposed a typical absorption profile with good detected absorption component in blue wing-P Cyg profile. For some dates, we can detect weak absorption component in the red wing of Hα. The emission peak is asymmetric and the peak mainly has positive radial velocity in range $+50 \div 60$ km/s, since bisector radial velocity RVbis (displacement of the line center at the level of the half intensity) shows mainly $\sim +30$ km/s values. As can be seen from Fig.1, emission components in the line Hβ has relatively weak intensity than in the line Hα. Emission component demonstrated double peak emission with clearly detected central absorption. Both of the line profiles, Hα and Hβ is showed variability from night to night.

In the Table 2 have presented some spectral parameters of the Hα line: Sp-spectral designation, where each spectra have got as average of two spectra, obtained in the same night in sequence. Next columns are ordinary and modified Julian Date (MJD) dates of observations, EW1a -equivalent

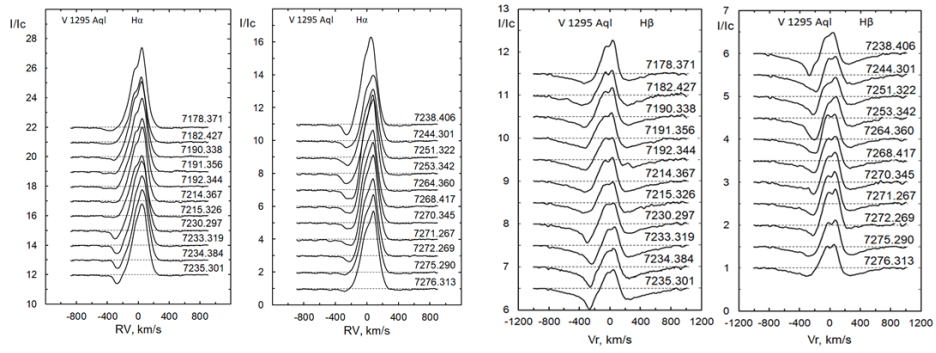

Fig. 1. All obtained profiles of the line Hα (left two panels) and Hβ (right two panels) in the spectrum V1295 Aql on the observations for 2015. Dates for each profiles in the figure presented in JD 2450000+

widths of the blue absorption component, EWe- equivalent widths of the emission component, EW2a –equivalent widths of the red absorption component, Ia1, Ie, Ia2 relative intensities of the same components, FWHMe - full width at half maximum of intensity of emission component, RVp- the peak radial velocities of the emission component, RVbis –bisector radial velocity of the emission component (the line center displacement at half of the central intensity). In the last two lines of Table 2 have presented mean values and rms (sigma) of these parameters. Spectral parameters of the line $H\beta$ is presented in the Table 3. In this table radial velocities of each components of the line central emission is presented: RV1p and RV2p are the emission component blue and red peaks radial velocities, RVa radial

Table 2. Some measured spectral parameters of the line $H\alpha$ in 2015.

Sp	Date	MJD	EW1a (Å)	Ewe (Å)	EW2a (Å)	Ia1	Ie	Ia2	FWHMe (Å)	RWp (km/s)	RWbis (km/s)
KS 6117-18	15.06 .04	57177.871	1.48	23.89	0.77	0.27	-4.13	0.14	4.66	62.2	27.56
KS 6156-57	15.06 .08	57181.927	1.04	21.15	0.36	0.17	-4.41	0.14	4.36	58.71	24.94
KS 6208-09	15.06 .16	57189.838	1.17	23.69	0.53	0.28	-4.79	0.12	4.96	54.97	24.73
KS 6224-25	15.06 .17	57190.856	1.89	22.7	0.44	0.2	-4.53	0.11	4.44	57.19	28.39
KS 6237-38	15.06 .18	57191.844	1.48	22.33	0.58	0.21	-4.4	0.09	4.53	58.92	29.9
KS 6439-40	15.07 .10	57213.867	1.45	24.17	0.61	0.11	-4.81	0.13	4.66	55.42	23.02
KS 6450-51	15.07 .11	57214.826	1.12	19.64	0.74	0.15	-3.96	0.09	4.5	54.78	18.56
KS 6530-31	15.07 .26	57229.797	2.14	22.35	0.54	0.58	-4.58	0.13	4.65	45.36	23.59
KS 6589-90	15.07 .29	57232.819	2.22	20.91	0.63	0.57	-4.6	0.1	4.42	47.64	30.44
KS 6607-08	15.07 .30	57233.884	2.67	20.81	0.48	0.58	-4.46	0.1	4.31	52.91	36.96
KS 6617-18	15.07 .31	57234.801	1.75	21.63	0.66	0.61	-4.71	0.09	4.6	50.01	28.44
KS 6670-71	15.08 .03	57237.906	1.86	24.02	0.6	0.67	-5.31	0.15	4.31	52.89	28.91
KS 6719-20	15.08 .09	57243.801	2.14	18.08	0.95	0.44	-3.87	0.12	4.64	75.2	49.73
KS 6818-19	15.08 .16	57250.822	2.72	18.75	0.72	0.52	-4.19	0.12	4.34	72.78	43.78
KS 6834-35	15.08 .18	57252.842	2.22	19.72	0.57	0.63	-4.56	0.13	4.27	70.08	40.08
KS 6870-71	15.08 .29	57263.860	2.1	24.6	0.4		-5.67		4.7	61.03	29.51
KS 6903-04	15.09 .02	57267.917	2.39	19.8	0.76	0.43	-4.37	0.14	4.49	58.48	20.4
KS 6937-38	15.09 .04	57269.845	1.21	22.85	0.09	0.33	-5	0.03	4.65	58.04	26.94
KS 6957-58	15.09 .05	57270.767	1.23	24.06	0.29	0.35	-5.3	0.07	4.6	60.23	27.39
KS 6974-75	15.09 .06	57271.767	1.06	21.79	0.17	0.37	-4.71	0.06	4.67	58.66	25.91
KS 7031-32	15.09 .09	57274.790	1.03	27.83	0.29	0.31	-5.87	0.06	4.89	58.64	24.69
KS 7060-61	15.09 .10	57275.813	1.1	22.07	0.6	0.17	-4.7	0.11	5.2	63.02	26.04
Mean			1.70	22.13	0.54	0.38	-4.68	4.59	4.59	58.51	29.09
Sigma			0.56	2.25	0.21	0.18	0.51	1.00	1.00	7.32	7.45

Table 3. Spectral parameters of the line $H\beta$ for 2015.

MJD	EW1a (Å)	Ewe (Å)	EW2a (Å)	Ia1	Ie	Ia2	FWHM(Å)	RV1p (km/s)	RV2p (km/s)	RVbis (km/s)	RVa (km/s)
57177.871	1.35	1.98	1.34	0.26	-0.7	0.23	3.07	-27.4	57.1	13.9	3.6
57181.927	1.01	1.96	1.25	0.21	-0.6	0.24	3.3	-32.8	51.0	-3.2	4.2
57189.838	1.21	2.12	1.25	0.26	-0.63	0.22	3.7	-47.3	44.0	-15.4	-6.2
57190.856	1.16	2.03	1.23	0.23	-0.59	0.22	3.81	-39.5	41.4	-23.3	-15.2
57191.844	1.26	1.85	0.9	0.24	-0.51	0.2	3.52	-29.8	52.8	-14.0	5.6
57213.867	1.34	1.79	1.22	0.26	-0.56	0.24	3.43	-61.4	30.9	-29.8	-22.5
57214.826	1.41	1.39	1.66	0.26	-0.43	0.26	3.65	-61.5	38.3	-24.6	-17.2
57229.797	1.7	1.61	1.1	0.44	-0.49	0.21	3.4	-26.3	44.7	-5.0	6.9
57232.819	1.44	1.48	1.28	0.43	-0.49	0.24	3.2	-24.5	43.9	1.6	1.6
57233.884	1.92	1.12	2.06	0.49	-0.39	0.28	2.8	-24.4	37.6	3.8	-7.5
57234.801	2.03	1.35	1.24	0.51	-0.49	0.25	3.2		33.2	-4.4	
57237.906	1.93	1.17	1.52	0.43	-0.43	0.27	2.84	-33.3	36.1	-3.5	-17.4
57243.801	1.92	1.21	1.18	0.39	-0.43	0.21	2.97	-31.0	45.6	8.6	-7.7
57250.822	1.89	1.21	0.94	0.43	-0.42	0.21	3.48		41.6	-4.0	
57252.842	1.93	1.36	1	0.51	-0.5	0.21	2.99	-37.5	48.1	12.1	-4.0
57263.860	1.64	1.63	1.12	0.33	-0.52	0.23	3.4	-61.7	26.4	-19.8	-19.8
57267.917	1.33	1.7	1.21	0.29	-0.5	0.22	3.4	-33.5	52.7	1.8	-2.1
57269.845	1.25	2.25	0.77	0.29	-0.7	0.18	3.6	-14.7	55.0	16.6	11.7
57270.767	1.18	2.42	0.73	0.27	-0.74	0.16	3.44	-55.1	29.0	-16.7	-20.4
57271.767	1.25	2.13	0.89	0.3	-0.64	0.2	3	-32.1	53.5	1.4	8.9
57274.790	0.92	2.13	1.02	0.21	-0.64	0.19	3.38	-39.8	47.4	-0.6	-0.6
57275.813	1.02	1.78	0.96	0.2	-0.53	0.18	3.66	-52.4	33.4	-16.5	-18.4
Mean	1.46	1.71	1.18	0.33	-0.54	0.22	3.33	-38.30	42.89	-5.50	-5.83
Sigma	0.35	0.40	0.31	0.10	0.10	0.03	0.30	14.29	8.53	12.83	11.10

velocity of the central absorption components. Other parameters in Table 3 are the same as in Table 2 for the line Hβ.

Figure 2 shows graphs illustrating changes in individual parameters of the Hα line. In Fig. 2, individual panels from left to right and from top to bottom shows the time variability in the following parameters: for dates JD 2457230-2455775 we have detected increasing of the parameters EW1a, decreasing of EWe and some red displacement in radial velocities of emission component of the line Hα. As can be seen from Fig.2, all these parameters are demonstrated variations with characteristic time nearly 45 days. The maximal amplitude of variation of the radial velocity of emission line is about 25 km/s. If we compare the profile variability of the Hα line with this interval of time variations, demonstrated in the Fig.1, we can make sure that increasing of intensity of blue absorption component and variation of measured spectral parameters occurred simultaneously. In the Fig1 we clear can see that starting from JD 2457230 blue absorption component in Hα emission is appeared.

Such structure in emission component is observed up to JD 2457275, total for 45 nights. Interestingly that variability of intensity versus wavelength of the emission component for parameter σ_2 (rms of intensity versus λ) shows double peak structure, which demonstrated that main variability in the structure of emission, occurred on the both blue and red wings of the line Hα (last panel in Fig.2). To make it easier to compare the values of σ_2 with the average intensity for the season, we formally added one to the values of σ_2. It is indicated that we have observed both ejection and fall of the matter in the circumstellar disc. This argument showed that rather in V1295 Aql we could see some signs of the matter accretion.

In the Fig. 3 have presented the diagrams, which illustrated time variability of some obtained parameters for the Hβ line. In the panels of Fig. 3 from left to right are presented parameters EW1a, If we look at the profiles of the Hβ lines, which are also shown in the Fig. 1, it is clear that the central emission is superimposed on the normal photospheric profile of the A star with wide Stark wings. Unlike Hα, the emission intensity in the Hβ line is weaker, so absorption components are clearly distinguished in both the blue and red wings of the emission. As can be seen from Fig.1, the blue and red borders of the emission peak and the entire Hα line at the continuum level have a displacement of $\pm 400 - 450$ km/s. If we measure the boundaries of the blue and red wings of the emission component of the Hβ line from the points of intersection with the photospheric wings, then here too the width of the emission component at the continuum level will be about 450 km/s. Of course, as in Hα, also in the Hβ line, an absorption component with non-photospheric nature can be most likely observed in the blue wing. However, this component cannot resolved from photospheric absorption in blue wing.

The FWHM of the emission component of the Hα line are $225 - 250$ km/s, and the line width at the level of 10% of the central intensity was obtained nearly

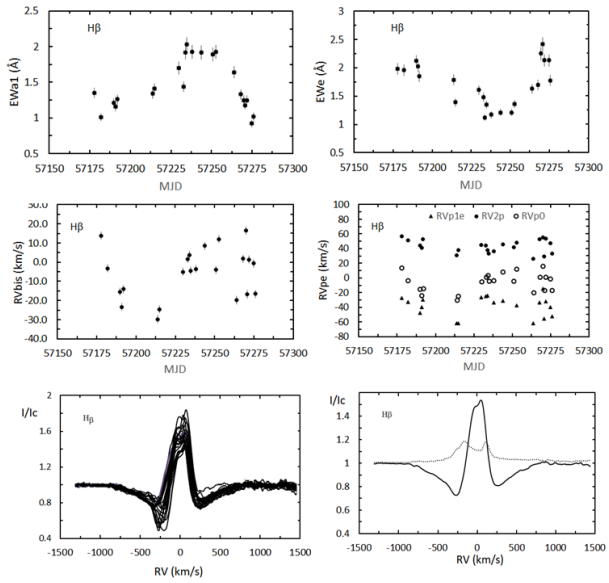

Fig. 2. Variation of spectral parameters (from Table 2) and profiles of the line Hα. In last panels presented superimposed line profiles (left) and average profile for the 2015. With dotted lines demonstrated rms (σ_λ) of intensity in wavelength. To make it easier to compare the values of σ_λ with the average intensity for the season, we formally added one to the values of σ_λ.

of 350 km/s. The maximum FWHM of the emission component of the Hβ line is $\sim$ 225 km/s, and the full width at the level of 10% of the central intensity, like that of the Hα line, is about 350 km/s. As is known, non-accreting objects exhibit narrow ($\Delta V \lesssim 230 - 270$ km/s) and symmetric line profiles of chromospheric origin, while accreting objects has wide ($\Delta V \gtrsim 230 - 270$ km/s) and asymmetric profiles [23, 25]. This is an argument indicating the existence of disk accretion in the star.

A comparison of the profiles of these two lines in the Fig. 1 showed that the absorption structure observed in the blue wing of the Hα line shows the outflow of gas from the disk, while the absorption in the blue wing of the Hβ line emission also has a contribution from the photospheric wing.

4. VARIABILITY OF SOME OTHER LINES

The He I 5876 line is observed as a weak and width emission, whose width at the continuum level reaches $850 - 900$ km/s. However, the FWHM of the line is the same as that of the Hα and Hβ hydrogen lines ($\sim$ 350 km/s). On certain dates, this line exhibits two peaks and a central dip, although more probable a

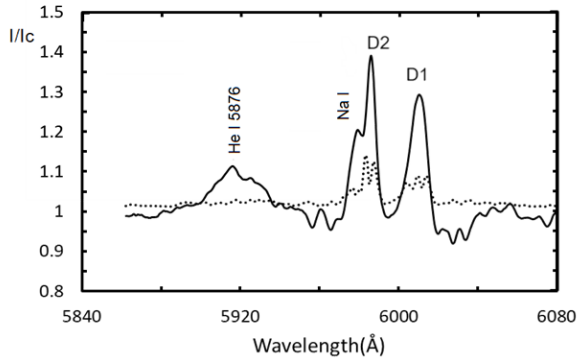

Fig. 3. Variation of spectral parameters (from Table 3) and profiles of the line $H\beta$. In last panels are presented superimposed line profiles (left) and average profile (right) for the 2015. With dotted lines demonstrated rms (σ_λ) of intensity in wavelength.

profile with one peak is observed. Figure 4 shows the average line profile for the lines He I 5876 and Na I D1, D2 averaged over the entire 2015 season. In the same place, the dotted line shows the intensity variation level (rms) in each wavelength, -92 . As can be seen, the central intensity of the He I 5876 line does not show any definite variability.

In the Table 4 is presented the measured parameters of the He I 5876 line. In the columns of Table 4 from left to right have shown the dates of observations in MJD, equivalent widths EW(Å), central intensities Ie, full width at half maximum FWHM (Å), radial velocities of the largest emission peak RVp(km/s), bisector radial velocity RVbis (km/s). To add the provided data to a 'longtable' with a caption and label in LaTeX, you can use the following code:

Table 4: Some measured parameters of the He I 5876 line.

MJD	EW (Å)	Ie	FWHM (Å)	RVp (km/s)	RVbis (km/s)
57177.871	1.05	-0.13		-44.46	-36.51
57181.927	0.48	-0.10	5.35	-39.74	-33.76
57189.838	0.49	-0.11	5.03	-43.84	-23.01
57190.856	0.59	-0.12	5.80	-40.80	-24.28
57191.844	0.84	-0.13	7.30	-41.00	-5.56
57213.867	0.50	-0.10	4.79	-45.69	-20.50
57214.826	0.45	-0.08	6.33	5.76	-25.43
57229.797	0.50	-0.10	6.99	-42.38	-10.12
57232.819	0.67	-0.10	6.90	-50.34	-19.00

MJD	EW (Å)	Ie	FWHM (Å)	RVp (km/s)	RVbis (km/s)
57233.884	0.89	-0.14	6.90	-41.78	-5.31
57234.801	1.01	-0.15	5.96	-38.48	4.43
57237.906	0.55	-0.13	4.93	-47.48	-28.49
57243.801	0.43	-0.14	4.32	-49.79	-20.86
57250.822	0.62	-0.14	6.00	-53.14	-24.37
57252.842	0.55	-0.12	5.28	-52.22	-18.52
57263.860	0.82	-0.18	6.47	-62.33	-24.56
57267.917	0.83	-0.13	6.82	-33.93	-15.69
57269.845	1.17	-0.14	6.62	-43.03	-30.77
57270.767	0.64	-0.09	6.40	-16.01	-10.25
57271.767	0.80	-0.10	6.53	-11.52	-34.61
57274.790	0.62	-0.11	6.48	-64.86	-26.52
57275.813	1.01	-0.14	7.50	-10.43	-24.80
Mean	0.71	-0.12	6.13	-39.43	-20.84
Sigma	0.22	0.02	0.88	17.14	10.34

The sodium doublet lines NaI D1, D2 are exhibit double peak emission with central absorption. In the Figure 4 next to the He I 5876 line we show the average D Na I line profiles for 2015. The dotted line there also shows variation in the parameter σ_2 along the wavelength. As can be seen, the maximal variations in both D1 and D2 lines is detected in the strongest red component, which also as a hydrogen emission lines exhibits double peaks in the σ_2 distribution.

In the Figure 5 is shown a graphs of time variations in the equivalent widths and bisector radial velocity of the He I 5876 line. As can be seen in Figure 4, in some nights there is a certain scatter around the average value, while in whole observation season 2015 the average value does not show significant variations in time. As can be seen in Fig.5, the He I and [OI] emission lines parameters show a weak scatter, in which the wave-like variability is not as clearly expressed as in the hydrogen and other lines.

5. SI II DOUBLET LINES 6347 AND 6371.

The Si II 6347 and 6371 lines are one of the most intensive and, in terms of their profile, typical spectral lines in the spectrum of the star. In the Figure 6 is shown the Si II doublet lines averaged over the 2015 season, as well as the forbidden line [OI] 6363. As can be seen, the line has a double emission peak with a deep and narrow central absorption. The dotted line shows variation in intensity along the spectral line. It can be seen that the greatest variations in intensity is observed in the central part of the line. As can be seen from Table 5, the blue and red components, respectively, have negative and positive velocities, and the central absorption shows RVbis close to the radial velocities of the stellar photosphere. At the continuum level, both emission components together

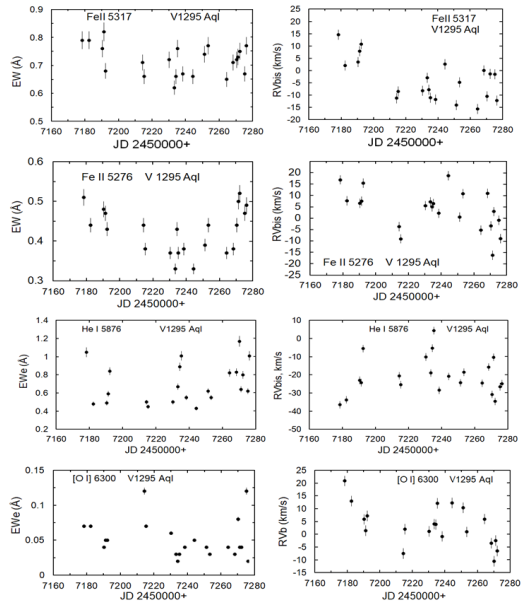

Fig. 4. From top to bottom time variations of the equivalent widh and bisector radial velocity of lines FeII 5317, 5276, He I 5876 and [OI] 6300.

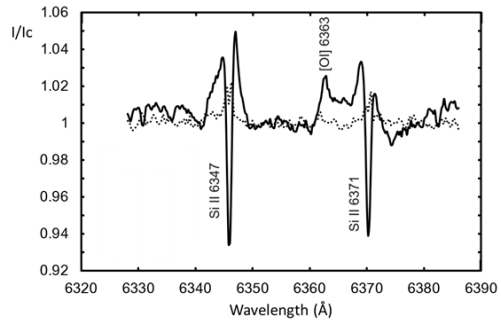

Fig. 5. Mean seasonal profiles of the He I 5876 and Na I D1,D2 emission lines for 2015. Dotted lines indicated variation level of intensity σ_λ along the spectral lines.

are expanded up to 350 km/s, and the FWHM of the central absorption corresponds to a vsini at $\sim$ 30-35 km/s. In the Figure 7 is shown time variations diagrams in some parameters used from Table 5. As can be seen from this figure, the largest variability have observed for the parameters of the blue emission component. Radial velocities for individual components also shows a variation in range from 5 (for absorption component) to 40 km/s (for blue emission component) for various components.

From Fig. 7 it is clearly seen that the variations in the parameters EW1e and RVbis in the range of dates MJD 57230-57270 exhibit a wave-like smooth variation with characteristic time scale of about 40 days. Note that a similar variation is clearly visible in

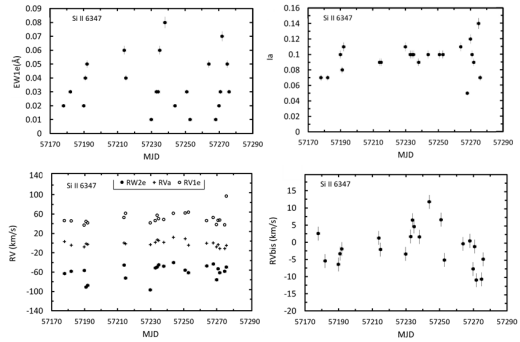

Fig. 6. Average line profiles of Si II 6347, 6371, as well as their standard deviation from the average σ_λ (dashed line).

the hydrogen emission lines Hα and Hβ. The data in the line Si II 6371 shows the same results as the Si II 6347 line. In the Figure 4 have shown graphs of time variations of

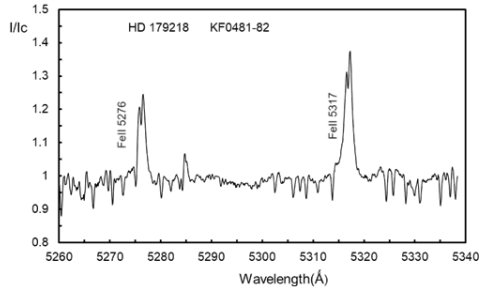

Fig. 7. Time variability of parameters of spectral line SiII 6347: from left to right and from top to bottom – EW1e, Ia, RV2e (open circles), RVa (crosses), RV1e (dark circles). In right panel RVbis for central absorption component for the line SiII 6347.

equivalent widths (left panels) and radial velocities (right panels) for individual emission spectral lines FeII 5317, 5276, HeI 5876 and [OI] 6300. The FeII lines exhibit smooth variations in the observed parameters. For lines, He I 5876 and [OI] 6300 obtained some level scatter of measured parameters around mean values.

The star's spectrum exhibit numerous lines of single ionized and neutral iron, most of which has double-peak profiles with weak central absorption. These are lines Fe II 5317, 5276, 4924, 4957, 5018, 5169, 5197 and others. A typical profile for a pair of lines FeII 5317, 5276 is shown in Fig. 7.

As can be seen, the line profile is mainly demonstrated an double peak emission with central absorption, and on some dates, weak narrow absorption components are detected on the blue wing. It is well known that similar profiles of emission lines of Fe II ions in the spectrum of a star has been observed in the flare spectrum of the solar chromosphere. Some measured parameters of the line Fe II 5317 presented in the Table 6. In the Fig.4

Table 5. Some spectral parameters of the line Si II 6347

MJD	EW1e Å	EWa Å	EW2e Å	Ie1	Ia	Ie2	RV1e	RVa km/s	RV2e km/s	RVbis km/s	FWHM Å
57177.871	0.02	0.05	0.03	-0.02	0.07	-0.03	-62.82	3.21	46.29	2.54	0.69
57181.927	0.03	0.05	0.01	-0.02	0.07	-0.02	-58.43	-4.26	45.95	-5.44	0.84
57189.838	0.02	0.07	0.03	-0.03	0.1	-0.04	-56.36	-7.91	36.9	-6.46	0.78
57190.856	0.04	0.06	0.04	-0.02	0.08	-0.05	-90.85	-1.71	44.78	-3.33	0.8
57191.844	0.05	0.1	0.03	-0.04	0.11	-0.03	-87.56	-2.47	41.44	-1.96	0.89
57213.867	0.06	0.05	0.05	-0.06	0.09	-0.05	-45.33	0.32	52.44	1.24	0.68
57214.826	0.04	0.08	0.01	-0.03	0.09	-0.01	-72.13	-1.28	61.11	-2.11	0.96
57229.797	0.01	0.09	0.03	-0.02	0.11	-0.03	-96.58	-3.39	41.73	-3.39	0.89
57232.819	0.03	0.08	0.01	-0.04	0.1	-0.02	-51.43	1.66	45.97	1.66	0.8
57233.884	0.03	0.06	0.06	-0.03	0.1	-0.05	-49.57	6.45	57.4	6.45	0.64
57234.801	0.06	0.06	0.03	-0.04	0.1	-0.04	-44.84	5.69	50.62	4.58	0.74
57237.906	0.08	0.06	0.02	-0.06	0.09	-0.02	-47.54	1.56	48.42	1.56	0.73
57243.801	0.02	0.08	0.03	-0.02	0.1	-0.04	-40.18	11.78	61.55	11.78	0.94
57250.822	0.03	0.09	0.03	-0.04	0.1	-0.03	-56.01	8.71	62.15	6.56	0.9
57252.842	0.01	0.08	0.01	-0.04	0.1	-0.02	-61.4	-4.48	63.76	-5.15	0.87
57263.86	0.05	0.08	0.02	-0.03	0.11	-0.03	-47.29	-0.45	46.32	-0.45	0.8
57267.917	0.01	0.03	0.03	-0.02	0.05	-0.03	-43.35	0.4	52.43	0.4	0.7
57269.845	0.02	0.08	0.04	-0.02	0.12	-0.04	-75.9	-7.76	38.12	-7.76	0.76
57270.767	0.03	0.07	0.08	-0.03	0.1	-0.07	-52.92	-3.01	46.83	-1.23	0.8
57271.767	0.07	0.05	0.09	-0.01	0.09	-0.05	-61	-11.45	47.34	-11.01	0.78
57274.79	0.05	0.11	0.01	-0.01	0.14	-0.02	-58.47	-11.59	37.48	-10.76	0.87
57275.813	0.03	0.04	0.07	-0.03	0.07	-0.06	-49.76	-4.93	96.89	-4.93	0.7
Mean	0.04	0.07	0.03	-0.03	0.10	-0.04	-59.53	-1.13	51.18	-1.24	0.80
Sigma	0.02	0.02	0.02	0.01	0.02	0.02	15.82	6.01	13.00	5.67	0.09

time variations of equivalent widths (left panels) and radial velocities (right panels) of the emission lines Fe II 5317, 5276 are presented. Both lines demonstrated large scatter

Table 6. Some spectral parameters of the line Fe II 5317.

MJD	EW(Å)	Ie2	FWHM(Å)	RV2e (km/s)	RVbis (km/s)
57177.871	0.79	-0.42	1.66	16.6	14.5
57181.927	0.79	-0.40	1.71	12.0	2.1
57189.838	0.76	-0.39	1.80	10.9	3.5
57190.856	0.82	-0.42	1.60	17.2	7.9
57191.844	0.68	-0.36	1.63	19.2	10.7
57213.867	0.71	-0.31	2.03	6.3	-11.3
57214.826	0.66	-0.29	1.95	1.1	-8.5
57229.797	0.72	-0.29	1.85	0.1	-8.2
57232.819	0.62	-0.27	2.06	11.9	-2.9
57233.884	0.66	-0.29	2.07	12.9	-7.8
57234.801	0.76	-0.30	2.30	8.9	-11.0
57237.906	0.67	-0.27	2.31	-13.4	-11.7
57243.801	0.66	-0.29	2.12	22.0	2.6
57250.822	0.74	-0.30	2.10	-8.7	-14.0
57252.842	0.77	-0.32	2.10	8.9	-4.7
57263.860	0.65	-0.30	1.85	-7.1	-15.6
57267.917	0.71	-0.30	2.20	13.2	0.1
57269.845	0.72	-0.30	1.96	4.5	-10.5
57270.767	0.73	-0.30	1.80	-10.9	-24.2
57271.767	0.75	-0.33	2.00	3.8	-1.4
57274.790	0.67	-0.31	1.94	2.2	-1.5
57275.813	0.77	-0.30	2.10	-9.8	-12.2
Mean	0.72	-0.32	1.96	5.54	-4.73
Sigma	0.05	0.05	0.20	10.35	9.32

of parameters from average value and smooth variation in time.
FWHM of these lines is nearly 1.8-2 Å(Table 6), so this equivalent to width 110-120 km/s. On the stellar continuum level these emission lines has maximal width at 200 km/s.

6. DISCUSSION AND CONCLUSIONS

Our long-term spectral observations of the star in 2015 made it possible to identify a number of new characteristics of the star's spectrum and features of spectral variability in the unusual Herbig Ae star V1295 Aql. Below we briefly list the main results that were obtained in our work using these data.

1. We were able to trace the progress of variations in the profiles and spectrophotometric parameters of the emission components of the Hα and Hβ hydrogen lines. It is shown that with an increase in the blue absorption component in the profiles of hydrogen lines, the variability of the star's spectrum increases, which indicates the existence at this moment of an increase in mass ejection from the star. In a time interval of 98 days of observations in 2015, synchronous variability was discovered in these lines with a characteristic time of about 40 days.

2. All other spectral lines showed a synchronous smooth variation in spectrophotometric parameters with the lines of hydrogen Hα and Hβ. For different lines, the magnitude of the amplitude of variations in different parameters differs.

3. Monitoring variations over time in the profiles of the emission components of the Hα and Hβ lines showed that the main variability in the lines occurs on the wings of individual components. The half-width (250 km/s) and full width (350 km/s) at the continuum level of the hydrogen emission lines probably indicate the existence of outflow and accretion of matter from the circumstellar disk.

4. It has been shown that the intensities of the lines He I 5876 and [O I] 6300, 6363 do not show significant variations versus time. Apparently, the He I 5876 line is formed in the stationary part of the disk, and the [OI] lines are formed in the outer rarefied part of the circumstellar disk. However, the weak synchronous variability of the [O] lines with the hydrogen lines indicates their sensitivity to the main mechanism of variability of the star's spectrum.

5. Lines D1, D2 NaI show double peak emission, with a dominant red component in intensity. The main variability in these lines is found only in the red wing. Since on some dates it is impossible to resolve the blue component in the D1 line, and the red component shows significant variability, this indicates the formation of these lines mainly in the zone of accretion of matter to the star.

6. Si II lines 6347, 6371 show a double emission peak with a deep central absorption, which has a width of 32 km/s, which significantly exceeds the rotation speed vsini $\sim$ 3.2 km/s obtained in the work of [3]. Perhaps this line component has an additional contribution from Boltsman expansion in a higher temperature environment (self-absorption).

7. FeII lines have a two-component emission peak with weak central absorption. This structure applies to most emission spectral lines. Perhaps the star has a powerful chromosphere, where similar spectral lines can form.

REFERENCES

1. Alecian E., Neiner C., Mathis S., et al., 2013c , A&A **549**, L8

2. Alecian E., Wade G. A., Catala C. et al., 2013b, MNRAS **429**, 1027

3. Alecian E., Wade G.A., Catala C. et al., 2013a, MNRAS **429**, 1001

4. Alicia N. Aarnio , John D. Monnier ., et al., 2017, ApJL, **18**, 34

5. Allen D. A., & Swings J. P., 1976, A&A, **47**, 293

6. Bahaddinova, G. R., Ismailov N. Z., Bashirova, U. Z.2020 , AzAJ **15**, 161

7. Bahaddinova, G. R.; Ismailov, N. Z.; Bashirova, U. Z. 2022, AzAJ **17**, 73.

8. Catala C., Alecian E., Donati J. F., et al., 2007, A&A, **462**, 293

9. Cauley, P. W., & Johns-Krull, C. M. 2014, ApJ, **797**, 112

10. Cidale L., Zorec J., & Morrell N., The Be Phenomenon in Early-Type Stars, 2000, ASP Conf. Ser., in IAU Colloq.175, **214**, 87

11. Corcoran, M., & Ray, T. P. 1998, A&A, **331**, 147

12. Cuttela M., & Ringuelet A. E., 1990, MNRAS, **246**, 20

13. de Winter D., van den Ancker M. E., Maira A., et al., 2001, A&A, **380**, 609

14. Hubrig S., Stelzer B., Scholler M., et al., 2009, A&A, **502**, 283

15. Hubrig S., Yudin R.V., Sch¨oller M., Pogodin M.A., 2006, A&A, **446**, 1089

16. Ismailov N.Z., Bahaddinova G.R.,Kalilov O.V., Mikailov Kh.M. 2013, Astrophys. Bull., **68**, 196

17. Ismailov, N. Z., Bashirova U. Z., Adigezalzade A. N. 2019, Astron.Bull.74, 300I

18. Lazareff B., et al., (2017),A&A **599**, A85,41

19. Malfait K., Bogaert E., & Waelkens C., 1998, A&A,, **331**, 211

20. Mikailov Kh. M., Khalilov V. M., and I. A. Alekberov, 2005, Tsirk. ShAO **109**, 21

21. Mikailova Kh. M., Musaev F. A., Alekberova I.A. et al., 2020, Kinematics and Physics of Celestial Bodies, **36**, No. 1, 22

22. Pogodin M.A., et al.,(2005), A&A **438**, 239

23. Ribas Á., Merín B., Bouy H., Maud L. T. 2014, A&A, 561, A54. Sitko M. L., 1981, ApJL, **247**, 1024

24. Sitko M.L., Astro.Jour., Part 1, 1981,vol. **246**, May 15, 161

25. Williams J.P., Cieza L.A. 2011, Ann.Rev.A&A, **49**, 67

26. Winter et al.,(2001), A&A **380**,609